Desalination and Water Treatment
www.deswater.com
doi: 10.5004/dwt.2018.23121

132 (2018) 120–133
November

Adsorption of phenol and p-chlorophenol from aqueous solutions on the template-synthesized mesoporous carbon

Yuzhen Li*, Ning Zhang, Zhen Li, Xiaojin Wang

College of Environmental Science and Engineering, Taiyuan University of Technology, 79 Yingze Street, Yingze District, Taiyuan, 030024, China, email: liyuzhen@tyut.edu.cn, liyuzhen123456@126.com (Y. Li)

Received 24 December 2017; Accepted 12 September 2018

ABSTRACT

The template-synthesized mesoporous carbon (TSMC) was prepared by nano-casting approach using KIT-6 as the template, sucrose as the carbon precursor, subsequently carbonized at the temperature of 900°C and then removal of the template. Phenol and p-chlorophenol were selected as the objectives to research the adsorption ability of the TSMC towards phenols. The effects of adsorbent dosage, pH, contact time, initial concentration and temperature were investigated using a batch technique. The results showed that the TSMC had significant adsorption capacity on phenol (21.13 mg/g) and p-chlorophenol (44.111 mg/g) under the optimum conditions: the dosage of 0.2 g and 0.1 g for phenol and p-cholorophenol, the initial pH 6.80 and 6.70 for phenol and p-chlorophenol, respectively, the equilibrium time of 120 min, the solution concentration of 100 mg/L and the adsorption temperature of 30°C. The adsorption kinetic studies demonstrated that the adsorption of phenols followed pseudo-second-order kinetic model. The best-fitted adsorption isotherm model was well fit using the Langmuir isotherm model. Besides, the thermodynamic parameters indicated that the adsorption process was spontaneous and endothermic. The π-π interaction, the hydrophobic interaction, the molecular dimensions, H-bonding and Electrostatic interaction were the possible mechanisms for phenols removal.

Keywords: Template-synthesized mesoporous carbon; Adsorption; Phenol; P-chlorophenol

1. Introduction

Phenols, as a result of various industrial activities such as pesticides, refineries, disinfectants, paints, plastics, drugs and wood preservatives plants [1–3] have been discharged into the environment. More seriously, phenols also endanger human health by food chain accumulation due to their high toxicity, mutagenicity, carcinogenicity and resistance to biodegradation [4]. Hence, in order to protect environment and human health, it is essential to study the rational and efficient treatment of phenols.

Various methods like biological (activated sludge method and MBR), physical (solvent extraction, membrane filtration and adsorption) and chemical (photo-catalytic degradation, advanced oxidation and electrochemical oxidation) technologies have been developed to apply for the remove of phenols from wastewater [5–7]. Among these techniques, adsorption is a simple, effective and time-saving technology for the removal of pollutants, in which the key factor is the exploitation of simplicity, efficiency and economy adsorbents.

In recent years, various materials have been employed by many researchers for the removal of phenolic compounds from wastewater as shown in Table 1 along with the values obtained in the present study [8–16]. Compared to the different adsorbents, the mesoporous carbons which possess a large specific surface area, accessible porosity, chemical inertness and good mechanical stability, gradually have attracted the global interest for and applications [17,18]. The mesoporous carbons possess pore size between 2.0 nm and 50 nm. However, the adsorption behavior of the mesoporous carbons for small molecular size organic pollutants, such as phenol and p-chlorophenol are often hindered due to the overlarge pore size. Therefore, the

*Corresponding author.

Table 1
Comparison of the adsorption capacity for the phenols onto various materials

Adsorbent	Adsorbate	Adsorption conditions (adsorbent dose, contact time temperature, pH)	C_0 (mg/L)	q_e (mg/g)	Reference
Hydroxyapatite nanopowders	Phenol	4 g/L, 4 h, 20°C, pH 6.4	100	6.47	[8]
Organoclay	p-chlorophenol	30 g/L, 1 h, 23°C, pH 5.0	100	12.09	[9]
Chitosan-calcium alginate blended beads	Phenol, p-chlorophenol	1 g/L, 4 h, 25°C, pH 7.0	100	71.40, 50.80	[10]
Schizophyllum commune fungus	phenol, p-chlorophenol	2 g/L, 3 h, 25 ± 2°C, pH 5.0	100	42.00, 48.00	[11]
Cu-nano zeolite	2-chlorophenol	4 g/L, 2.5 h, 20± 1°C, pH 6.0	100	49.02	[12]
Diethylenetriamine-modified activated carbon	Phenol	2–10 g/L, 1–4 h, pH 3.0–11.0	100–200	18.12	[13]
Biosorbent (CS/CA blended beads)	p-chlorophenol	0.4 g/L, pH 7.0	50–300	127	[14]
Bioadsorbent	Phenol, 2-chlorophenol , and 4- chlorophenol	0.05 to 0.8 g, 120 min, pH 6.0	50– 200	142.85, 204.08, 263.15	[15]
Biosorbent	Phenol, 2-chlorophenol and 4- chlorophenol	4 g/L, 4 h, pH 7.0	100–400	94.33, 147.05, 181.81	[16]
Template-synthesized mesoporous carbon	Phenol	4 g/L, 2 h, 30°C, pH 6.80	100	21.13	This study
Template-synthesized mesoporous carbon	p-chlorophenol	2 g/L, 2 h, 30°C, pH 6.70	100	44.11	This study

suitable pore size of the mesoporous carbon is essential. A number of reviews and perspective articles have demonstrated about the adsorption of phenols by the mesoporous carbons. Thus, Wei Teng et al. have employed ordered mesoporous carbons with pore size (2.6–3.8) nm prepared from the surfactant-templating method to remove contaminants [19]. In another study, Aibing Chen have investigated mesoporous carbonaceous materials with a uniform pore size 5.1 nm prepared from used cigarette filters for phenol adsorption, as well as exhibiting a considerable adsorption capacity [20]. Jianwei Fan et al. have been synthesized the ordered mesoporous carbonaceous materials with unique mesoporous size from 2.8 to 5.8 nm by the organic-organic self-assembly method with phenolic resin and F127 to remove Hexchlorobenzene [21].

Jie Yang et al. investigated that the mesoporous carbons from waste polyester possess an average pore width of 3.66 nm was beneficial for the adsorption of phenol [22]. In addition to, the functionalization of mesoporous carbonaceous materials (N-Fe/OMC) with pore size 3.8 nm were applied to remove phenol by Yang et al. [23]. The hollow mesoporous carbon spheres (HMCSs) with uniform mesoporous size (4.1 nm) exhibit a greater capacity for phenol adsorption [24]. Therefore, the small pore size mesoporous carbons seem to be more attractive candidates as adsorption materials for phenols. And the template-synthesized mesoporous carbon is relatively promising material, owing to its narrow pore size distribution and regulable pore structure [25].

So far as, the template method has been widely used to prepare various mesoporous carbons. There are three stages in the synthesis of the mesoporous carbon [18]: (1) the infiltration of the pores of the template with appropriate carbon precursor, (2) the carbonization of the carbon precursor, (3) the template removal. Thus, the pore size distributions and topology of pores of the prepared carbon material can be controlled by the pore structure of the template. Obviously, it is the key to choose the suitable template. Many kinds of templates could be applied in studies, such as SBA, KIT, HMS, MCM, various types of zeolites, clay, and attapulgite and so on [26,27]. In particular, the mesoporous silica templated KIT-6 consists of two interwoven mesoporous subnetworks with a right pore diameter, are more attractive for adsorption phenols [28].

In this paper, the template-synthesized mesoporous carbon(TSMC) was synthesized using KIT-6 as a template, sucrose as a carbon precursor. In addition to, the TSMC materials were characterized by means of BET, XRD and TEM, which showed that the sample was a worm-like disorderly mesoporous structure. To research adsorption abilities of mesoporous carbon towards phenols for developing the high-performance adsorbent, we have selected phenol and p-chlorophenol as the objectives. Batch adsorption experiments were systematically performed to study effect of adsorbent dosage, pH, contact time, initial concentration and temperature. Furthermore, we also evaluated the adsorption kinetics, the adsorption equilibrium isotherms, the adsorption thermodynamics and the adsorption mechanism.

2. Materials and methods

2.1. Materials

The KIT-6 and sucrose were purchased from College of Chemistry and Chemical Engineering, Bohai University. The phenol was purchased from Chemical reagent corporation (Tianjin, China). The p-chlorophenol was purchased from J&K Scientific Co., LTD (Beijing, China). HCl, H_2SO_4, NaOH HF (10%) were purchased from Chemical reagent

corporation (Tianjin, China). Deionized water was used in all experiments. All the chemicals were A.R. grade and used without further purification.

2.2. Synthesis of the template-synthesized mesoporous carbon

The template-synthesized mesoporous carbon was prepared as follows: Firstly, 2.0 g of KIT-6 was dissolved in 10 kg of Deionized water. Secondly, 2.5 g of sucrose and 0.28 g of sulfuric acid were added into the KIT-6 solution under stirring. All of the operations were performed at room temperature (20±2°C). After stirring for 24 h, then dried at 80°C for 4 h and 140°C for 6 h, respectively. Next, the obtained product was mixed with aqueous solution (1.5 g sucrose/10 g H_2O/0.16 g H_2SO_4) once again, and repeated the above process. The composite was calcined in N_2 atmosphere by slowly increasing 900°C for 4 h. Subsequently, the sample was dipped into HF (10 wt%) aqueous solution at room temperature for 24 h for twice to remove the silica matrix, washed with 500 mL of deionized water until the neutral pH and dried in air. Finally, the black and powder mesoporous carbon was denoted as the TSMC.

2.3. Characterization of the TSMC

X-ray diffraction (XRD) patterns of the TSMC were characterized by Powered X-ray diffractometer (XRD-6000, Japan) using CuKα (λ = 0.15425 nm) radiation operating at 40 kV and 30 mA with a scanning rate of 0.2°/s over the range of 0.6°–8°. Meanwhile, the crystal structures of the adsorbate were recorded in the range of 2θ from 5° to 70°. Transmission electron microscopy (TEM) measurements were conducted on a FEI F20 microscope (USA) operated at 200 kV, revealing the morphology and size of the TSMC. Before the characterization, the sample was dissolved in 20 mL ethanol solution and scattered ultrasonic for 30 min at room temperature. Then, the dispersion solution was covered on the carbon surface of copper net until the sample was desiccated. Surface area and pore analyses were performed using a Micromeritics ASAP 2020 system. The specific surface area was calculated from the desorption datas using the conventional Brunauer-Emmett-Teller (BET) method. The total pore volume was measured from the amount of N_2 adsorbed at a relative pressure of 0.99. The mesoporous volume, pore size distribution and pore diameter were estimated from the desorption branch of the isotherm using the Barrett-Joyner-Halenda (BJH) method. Before the TSMC determined by the N_2 adsorption/desorption isotherm at –196°C, the prepared sample was degassed at 80°C for 3 h until the mass attained a constant value. The surface functional groups on the TSMC were identified using a Fourier transform infrared spectrometer (NICOLET iS10, America) in the range of 4000–400 cm^{-1}. The sample was prepared by the KBr method.

2.4. Adsorption experiments

The adsorption behaviors of the phenol and p-chlorophenol on the TSMC were measured according to the following procedure. Typically, 0.2 g and 0.1 g mesoporous carbon were introduced into flasks containing 50 mL of 100 mg/L phenol and p-chlorophenol solutions, respectively, which were then shaken (180 rpm) for 2 h at initial pH and 30°C, respectively. After mixing, the solutions were filtered and analyzed using a UV spectrophotometer at a maximum wavelength of 270 nm for phenol and 280 nm for p-chlorophenol, respectively. At the same time, the effects of adsorbent dosage, the solution pH, contact time, initial concentration and contact temperature were investigated. The phenol or p-chlorophenol uptake at equilibrium q_e (mg/g) and the percentage of removal (%) were calculated by the following equations:

$$\text{Remove}(\%) = \frac{c_0 - c_e}{c_e} \times 100 \quad (1)$$

$$q_e = \frac{c_0 - c_e}{m} \times V \quad (2)$$

where c_0 and c_e (mg/L) are the initial and equilibrium concentration, respectively. V (mL) is the volume of the solution, and m (g) is the adsorbent dosage.

2.5. Regeneration experiments

Regeneration experiments for the TSMC were conducted as followings: (1) 0.2 g and 0.1 g of TSMC were put into 50 mL phenol (100 mg/L) and p-chlorophenol (100 mg/L), respectively, to adsorb phenols at 30°C for 120 min. (2) TSMC, which had adsorbed phenol and p-chlorophenol, were placed in ethanol with agitation about 4 h, respectively. And then, the filtrate was analyzed by UV/vis spectroscopy at a wavelength of 270 and 280 nm, respectively. (3) TSMC were washed with deionized water until neutral, followed by oven drying at 30°C and then used for the adsorption-desorption cycles. The procedure was repeated three times to study the sustainability of the TSMC.

3. Result and discussion

3.1. Characterization of the template-synthesized mesoporous carbon

To investigate the structure of the TSMC, the XRD profiles of the materials obtained in the small range are presented in Fig. 1, and the corresponding the wide-angle XRD pattern was inset. As can be seen from Fig. 1, the XRD pattern of TSMC reveals a peak which is not obvious at 2θ≈1° corresponding to the plane (211). Besides, the inset in Fig. 1 shows the wide-angle XRD pattern of the present materials at diffraction angles between 5 and 70°. The two broad peaks located at around 26.622° and 43.981° are referred to the characteristic carbon (002) and (100) diffractions, respectively, indicating the presence of long-range two-dimensional ordering in the carbon matrices [29]. Obvious distinction in the full width at half maximum (FWHM) of the (002) and (100) reflections implies the different crystallite sizes of the sample [30]. This is in agreement with a disorder structure of amorphous carbons.

In order to visualize the surface morphology of the TSMC, the transmission electron micrograph of the materials is shown in Fig. 2. It could be seen that the images of the TSMC show a less ordered mesoporous structure,

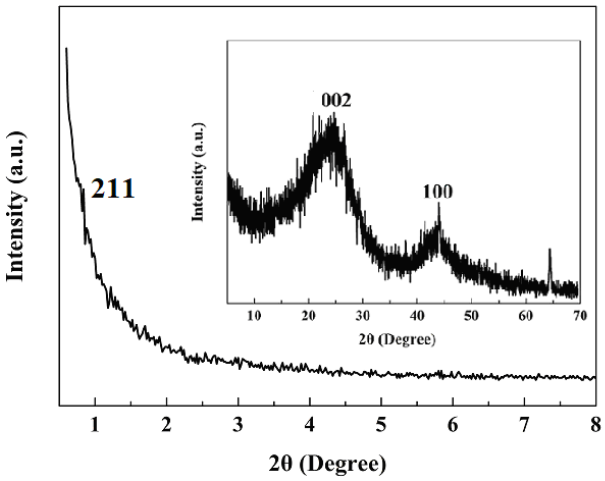

Fig. 1. The low-angle XRD pattern of the TSMC and the wide-angle XRD pattern of the TSMC (the insert).

which might be attributed to incompletely carbonization of polymerization sucrose [31]. As shown in Fig. 2A, it could be seen that the TSMC presents a worm-like disorderly pore structure, which is consistent with the results of the low angle XRD pattern. Besides, another phenomenon noted is that narrow slit-like pores are formed by the layered structure in Fig. 2B.

The porosity properties of the TSMC are revealed by examining the N_2 adsorption-desorption isotherms and pore size distributions. In Fig. 3 it is noted that the isotherm rises very sharply at low relative pressure, and reaches a high adsorption volume. It also can be showed a type-IV curve with a H_4-type hysteresis loop at high relative pressure according to the IUPAC classification, indicating that the slit-like pores are formed by the TSMC. During the carbonization, the sucrose lost most of its hydrogen, oxygen and few carbon elements in the form of gaseous evolution, thus more mesoporous were formed in the TSMC as shown in TEM morphology. In addition, the pore size distributions curve calculated from desorption branches by BJH model clearly confirm their narrow pore size of the maximum peak centered at about 3.8 nm (see the insert). The textural parameters of the TSMC are also calculated according to the isotherms of the sample. In detail, the TSMC reveals the surface area of 398.7667 m^2/g (BET surface area), the pore volume of 0.078128 cm^3/g and the pore size of 4.1350 nm (BJH Desorption average pore diameter (4V/A)). These results demonstrate that the TSMC exhibits hierarchical porous texture consisting of mesoporous acting as the more efficient adsorptive sites or charge storage. In this architecture, the TSMC is expected to provide favorable performance in adsorption of phenol and p-chlorophenol.

The FT-IR spectrum was used to characterize the existence of the surface functional groups of the TSMC. Fig. 4 shows the FT-IR spectra of the TSMC. A broad band at around 3430 cm^{-1} is observed in the sample, which may be caused by the -OH stretching vibration of the adsorbed water molecules. The band appeared at 1618 cm^{-1} is caused by the stretching vibration of the C=C double band. In addition, the C-O stretching vibration can be found around 1062 cm^{-1}. These results confirm that the enriched functional

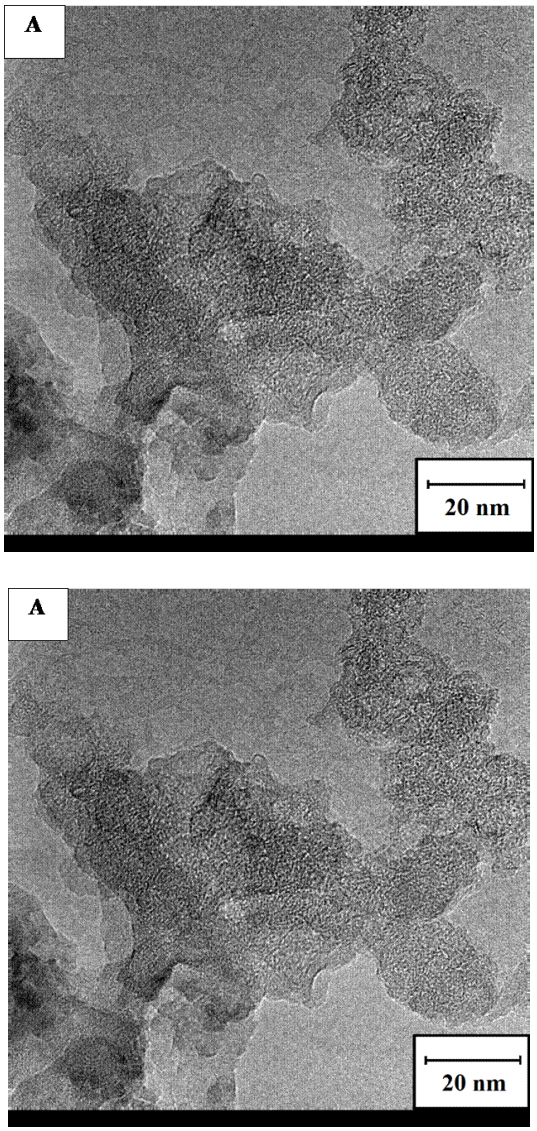

Fig. 2. TEM images of the TSMC, A (20 nm) and B (100 nm).

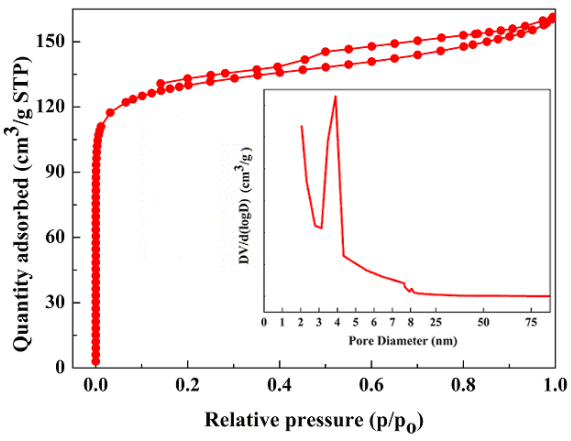

Fig. 3. Nitrogen adsorption-desorption isotherm of the TSMC and The BJH pore size distributions of the TSMC (the insert).

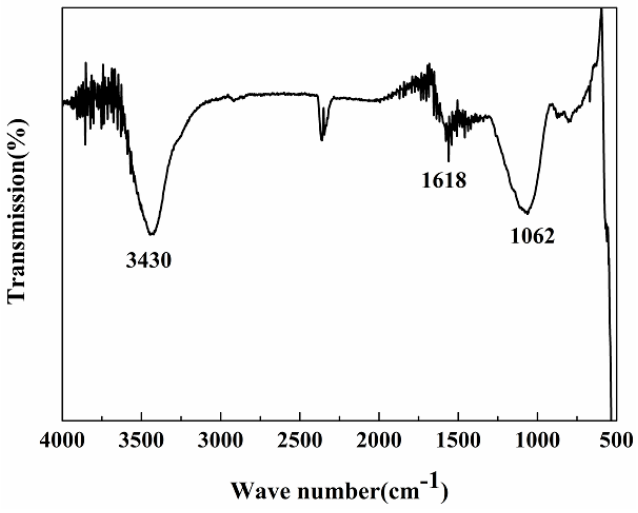

Fig. 4. The FT-IR spectrum of the TSMC.

groups of TSMC will make a contribution to the adsorption capacity for the phenols onto the TSMC. And the similar FT-IR results were also reported by Lang et al. [31].

3.2. Effect of adsorbent dosage

Influence of adsorbent dosage on removal degree of phenol and p-chlorophenol presented in Fig. 5. Similar trend for phenol and p-chlorophenol is noticed. It is observed from Fig. 5A, the percentage removal of phenol increases from 70.16 to 90.89% while the adsorption capacity decreases from 35.07 to 15.15 mg/g as the dosage of the TSMC increases from 0.10 to 0.30 g. And from Fig. 5B, it also can be found that the removal of p-chlorophenol increases from 31.31 to 90.41%, but the adsorption capacity decreases from 78.29 to 30.14 mg/g with the adsorbent loading up from 0.02 to 0.15 g. This phenomenon is partly because of the availability of larger surface area and more adsorption sites increasing with the adsorbent dosage, resulting in a higher removal percentage [3]. However, when the adsorbent dosage is over 0.3 g (phenol) and 0.15 g (p-chlorophenol), respectively, the removal percentage of phenol and p-chlorophenol rise only slightly, which clearly show the adsorption process reaching the saturated state.

From Fig. 5 it also can be found that the TSMC exhibits more specific adsorption ability for p-chlorophenol than phenol. Besides many functional groups with the mesoporous carbon according to the FT-IR characterization of the TSMC, nucleophilic Cl atom of p-chlorophenol may play a very important role during the adsorption process. Cl, O and H atoms of p-chlorophenol can be also form hydrogen bonding with functional groups of the TSMC. Therefore, there are large amount of p-chlorophenols on the surface of mesoporous carbon. However, as for phenol, the sole hydroxyl can been formed between phenol and the mesoporous carbon; Besides, the attraction from water molecules to phenol molecules is stronger than p-chlorophenol molecules because of the more hydrophilic of phenol, which result in that phenol has higher the adsorption capacity onto the TSMC than p-chlorophenol [32].

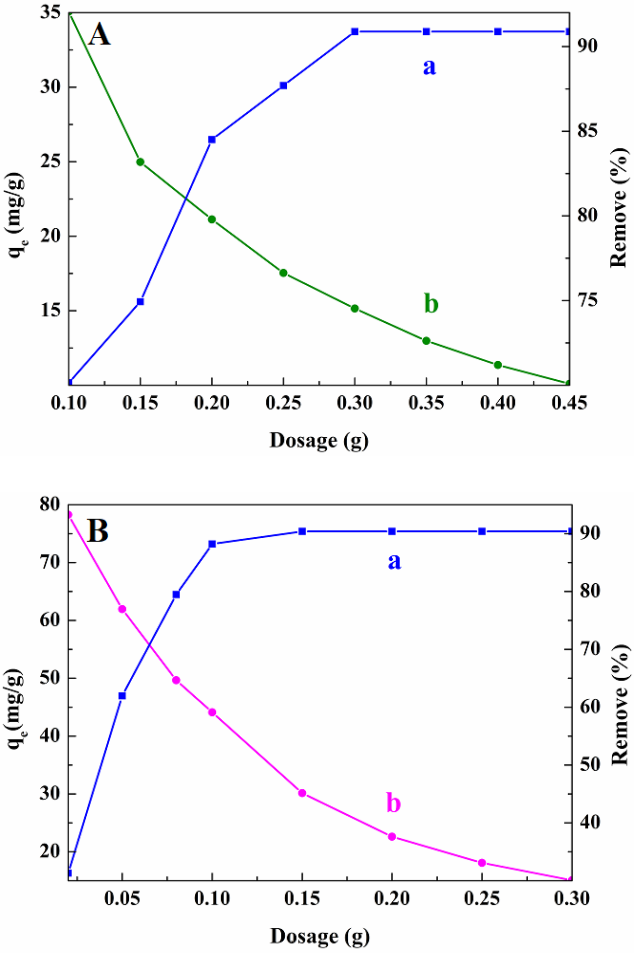

Fig. 5. Effect of the TSMC dosage on the adsorption of (A) phenol and (B) p-chlorophenol (a: The adsorption capacity q_e (mg/g), b: The removal rate (%), c_0: 100 mg/L, V: 50 mL, Temperature: 30°C, Contact time: 2 h, The initial pH 6.80 and 6.70 for phenol and p-chlorophenol, respectively).

3.3. Effect of the solution pH

The pH value of the solution is an important factor during the adsorption process, which can affect the structure the properties of both adsorbent and adsorbate [33,34]. The surface charge of the mesoporous carbon depends on the solution pH and its $pH_{PZC.}$ In general, the mesoporous carbon surface is positively charged at pH < pH_{PZC} and negatively charged at pH > pH_{PZC}. The adsorbate is mainly in protonated form at pH < pKa and in deprotonated form at pH > pKa.

Fig. 6 shows the effect of pH on the adsorption capacity of phenol and p-chlorophenol onto the TSMC. With increasing the values of pH, the adsorption capacity of phenols onto the TSMC do not change obviously at first. But when the value of pH exceeds 10.0 for phenol and 8.0 for p-chlorophenol, respectively, the adsorption capacity of phenols onto the TSMC sharply decrease. This behavior seems to be related to the pKa values of phenol and p-chlorophenol at 30°C are 9.89 and 9.41, respectively [35,36]. When the pH value of solution goes below the pKa value of phenols, phenols chiefly exist as molecules.

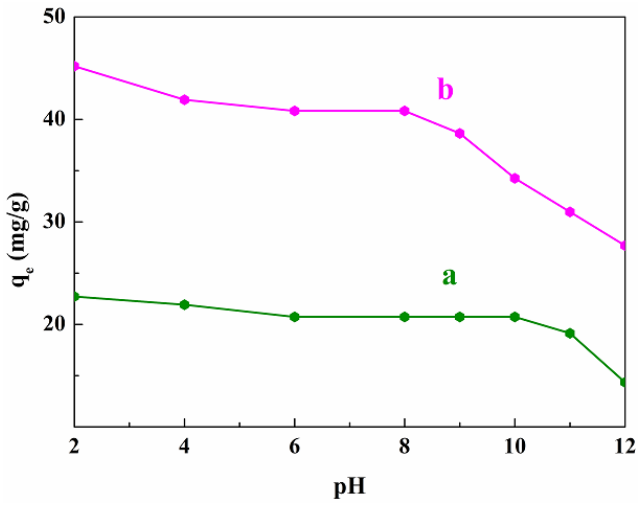

Fig. 6. Effect of pH on the adsorption of (a) phenol and (b) p-chlorophenol (c_0: 100 mg/L, V: 50 mL, Temperature: 30°C, Contact time: 2 h, Adsorbent dosage: 0.2 g for phenol, 0.1 g for p-chlorophenol, respectively).

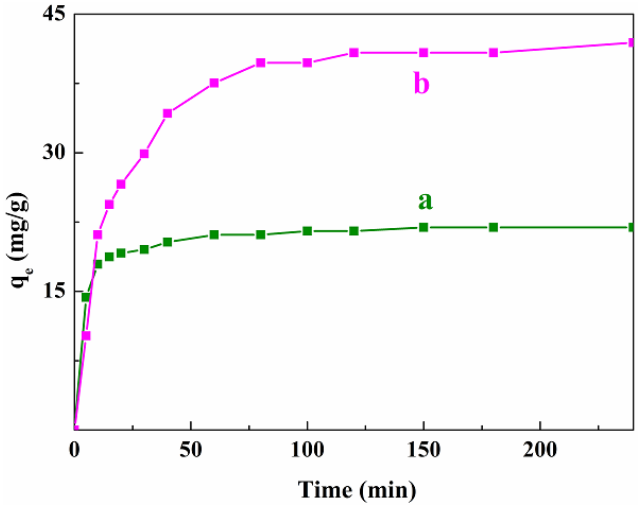

Fig. 7. Effect of the contact time on the adsorption of (a) phenol and (b) p-chlorophenol (C_0: 100 mg/L, V: 50 mL, Temperature: 30°C, Adsorbent dosage: 0.2 g for phenol, 0.1 g for p-chlorophenol, The initial pH 6.80 and 6.70 for phenol and p-chlorophenol, respectively).

Therefore, phenols effectively adsorbed onto the mesoporous carbon are molecules not phenolate anions. Thus, the molecular interactions including hydrogen bonding, hydrophobic interaction and Vander Waals forces are the possible factors for the adsorption of phenols onto the TSMC, especially the hydrogen bonding (According to the effect of adsorbent dosage). At pH > pKa, phenols chiefly exist as negative phenolate ions and the mesoporous carbon surface is negatively charged. Electrostatic repulsion force exists between the phenols and the mesoporous carbon surface.

With the increase of pH values up to 10.0, the phenols are dissociated to a higher degree and the mesoporous carbon surface is charged more negatively, and thus the electrostatic repulsion force occurs between them. Moreover, this effect also appears between the adsorbed phenolic anions ($C_6H_5O^-$ for phenol and $C_6H_4O^{-2}$, $C_6H_4OCl^-$, $C_6H_5O^-$ for p-chlorophenol, respectively) [37]. In addition, the dissociation of phenols also leads to a weakness of affinity between phenols and the surface of the TSMC [38].

3.4. Effect of the contact time and the kinetic study

In wastewater treatment applications, the contact time is an important parameter to determine whether the adsorption process reaches balance. Fig. 7 depicts the effect of contact time on the removal of phenols onto the TSMC. At the beginning, the curves rise sharply because the adsorption sites are initially abundant, and phenols are easily adsorbed on these sites. Additionally, the diffusion resistance is reduced to a large extent due to the open pore structure of the mesoporous carbon [39].

Eventually, a plateau reaches in the curves indicating that the adsorbent is saturated. This result is partly due to the fact that a number of available vacant adsorbent sites reduce with increasing contact time. As shown in Fig. 7, the phenols onto the TSMC exhibit different initial adsorption rates, which may be due to the molecular the widest molecular dimension. It was reported by authors that the molecular sizes of phenol and p-chlorophenol are 5.76 × 4.17(Å) and 6.47 × 4.17(Å), respectively [40]. Obviously, the p-chlorophenol has a larger widest dimension than phenol. The results are more consistent with the observations of other authors [41].

3.4.1. Adsorption kinetics study

The adsorption kinetic, which dictates residence time of the adsorption process, is one of the most important tools to assess the adsorption efficiency [42]. In order to explain the phenols adsorption mechanism onto the mesoporous carbon, adsorption kinetic studies are tested by the pseudo-first-order, pseudo-second-order, and intra-particle diffusion model in Fig. 8, and the kinetic parameters including the experimental and calculated adsorption capacity (q_e) are listed in Table 2. The pseudo-first-order model is given by the following equation [43]:

$$\ln\left(q_e - q_t\right) = \ln q_e - k_1 t \tag{3}$$

where k_1 (1/min) is the pseudo-first-order rate constant, q_e (mg/g) and q_t (mg/g) are the adsorption capacity of the adsorbent at equilibrium and at time t, respectively.

The pseudo-second order model is defined as the following equation [44]:

$$\frac{t}{q_t} = \frac{1}{k_2 q_e^2} + q_e t \tag{4}$$

where k_2 (g/mg/min) is the pseudo-second-order rate constant.

The adsorption process of the adsorbate molecules from the liquid phase onto the adsorbent surface is presumed to involve three stages: (1) the external boundary layer diffusion process, (2) intra-particle diffusion within the pores of

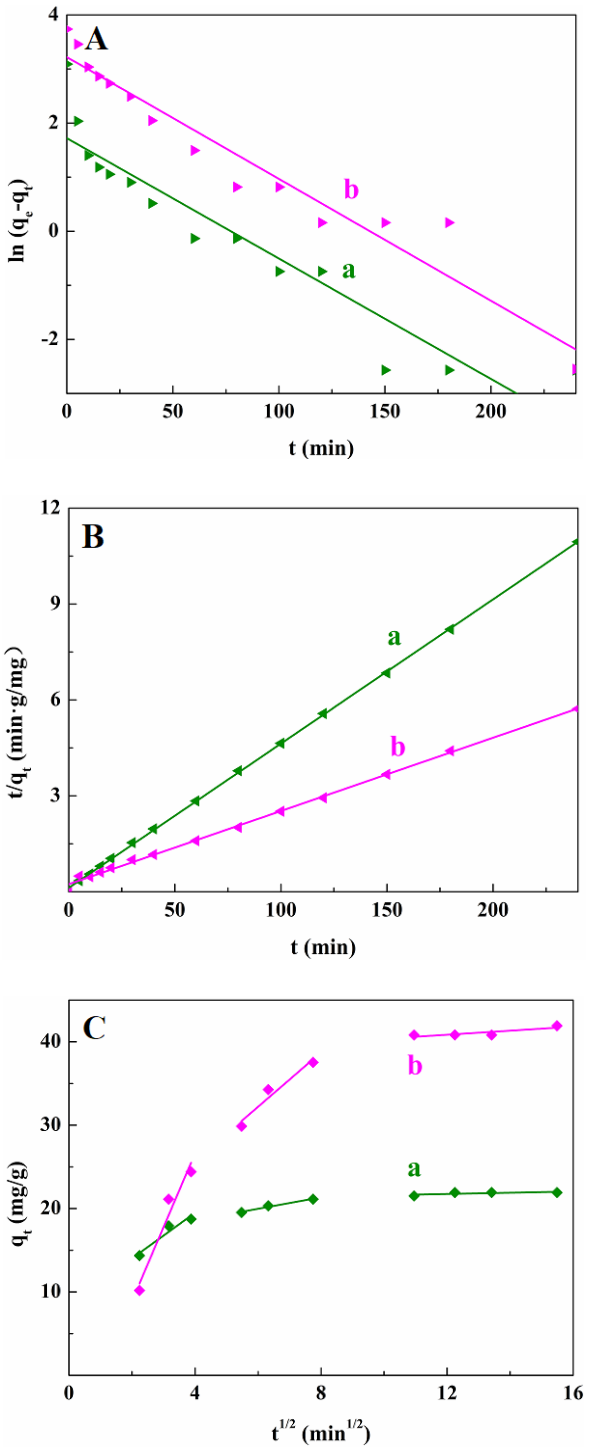

Fig. 8. Adsorption kinetic models of (a) phenol and (b) p-chlorophenol onto the TSMC A) the pseudo-first-order, B) the pseudo-second-order, C) the intra-particle diffusion model.

the adsorbent, (3) adsorption and desorption equilibrium process. The intra-particle diffusion model is represented by the following equation [45]:

$$q_t = k_3 t^{\frac{1}{2}} + C \quad (5)$$

Table 2
Kinetic parameters for phenols adsorption onto the TSMC

Kinetic type	Kinetic parameters	Phenol	p-chlorophenol
Pseudo-first-order	k_1 (1/min)	0.0223	0.0225
	$q_{e,\,cal}$ (mg/g)	5.595	25.068
	R^2	0.872	0.934
Pseudo-second-order	k_2 (g/mg/min)	0.0163	0.002
	$q_{e,\,cal}$ (mg/g)	22.168	43.668
	$q_{e,\,exp}$ (mg/g)	21.126	44.111
	R^2	0.9998	0.997
Intraparticle diffusion	C (mg/g)	15.842	12.613
	k_3 (g/mg/min$^{1/2}$)	0.689	3.266
	R^2	0.958	0.898

where k_3 (g/mg/min$^{1/2}$) is the intra-particle diffusion rate constant and C (mg/g) is a constant related to the bounding layer thickness [46].

As shown in Table 2, the pseudo-first-order model gives poor fitting with low R^2 values and notable variances between the experimental and theoretical uptakes. However, for the second-order-kinetic model, the R^2 values (0.9998 for phenol, 0.9973 for p-chlorophenol) are close to unity. Moreover, the similar values of experimental and calculated values of q_e (22.1680 mg/g for phenol, 43.6681 mg/g for p-chlorophenol) confirms a good agreement with this adsorption model. Therefore, the adsorption of phenols onto the mesoporous carbon fit with utmost accuracy the pseudo-second order model.

The curve-fitting plots of intra-particle diffusion model are demonstrated in Fig. 8C. It can be seen that the similar adsorption kinetic study for phenol and p-chlorophenol onto the TSMC, and the adsorption process can be divided into three sequential stages: a sharp rise stage, a less-sharp rise stage and a plateau stage. The initial sharp rise portion represents the external layer diffusion process restricted mainly by the pore structure of the mesoporous carbon; during the following less-sharp rise stage, the intra-particle diffusion is retarded mainly by the formerly adsorbed molecule process; the plateau portion corresponds to the final equilibrium process [45]. Moreover, the values of the intercept C (15.8423 mg/g for phenol, 12.6129 mg/g for p-chlorophenol, respectively) are not the zero point, which shows that the adsorption rate-controlling step is not only the intra-particle diffusion [5].

3.5. Effect of initial concentration and the isotherm study

In order to determine the effect of initial concentration on the adsorption of phenols on the mesoporous carbon, the solution with various initial concentrations (20–400 mg/L) were prepared. The results are shown in Fig. 9. The equilibrium adsorption capacity of phenols onto the TSMC rise sharply with initial concentration range from 10 to 160 mg/L, because the initial phenols concentration provides an important driving force to overcome all mass transfer resistances between the aqueous and solid phases [8]. However, when the initial concentration varies from 160 to 400 mg/L,

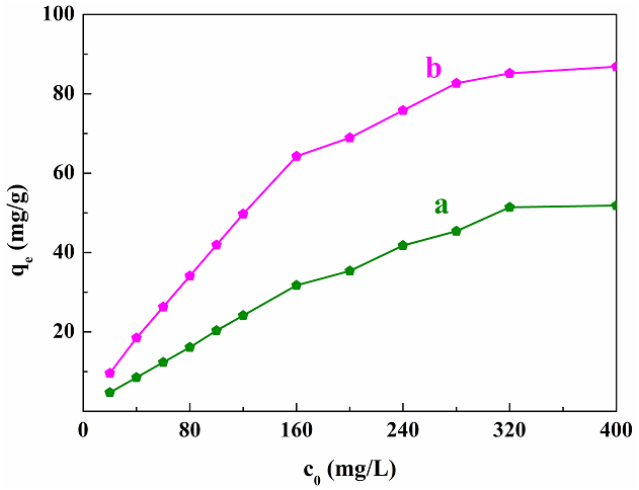

Fig. 9. Effect of the initial concentration on the adsorption of (a) phenol and (b) p-chlorophenol (*V*: 50 mL, Temperature: 30°C, Adsorbent dosage: 0.2 g for phenol, 0.1 g for p-chlorophenol, The initial pH 6.80 and 6.70 for phenol and p-chlorophenol, respectively).

q_e values increase more slowly and reach a plateau. This may be due to the increasing of mesoporous diffusivities [47]. In detail, as the initial adsorbate concentration in bulk increases, phenols diffusion of the mesoporous is gradually dominated, and boundary layer diffusion of phenols is weaken [48]. From Fig. 9 it is observed that p-chlorophenol onto the TSMC demonstrates higher adsorption capacity than phenol at the initial concentration of 20–400 mg/L. This behavior is partly due to the molecular size of phenol being smaller than the p-chlorophenol's. Similar results were reported by Liu et al., implying that only a small part of the mesoporous adsorb phenol, but as for substituted phenols, the phenomenon of adsorption is more evident [41].

3.5.1. Adsorption equilibrium isotherm study

The adsorption isotherm studies are very important for the optimization of the adsorption system. In this study, four classical adsorption isotherm models: Langmuir [49], Freundlich [50], Dubinin-Radushkevich (D-R) [51] and Temkin isotherms [52] are employed to describe the equilibrium data of phenols adsorption on the mesoporous carbon.

The Langmuir isotherm model is valid for monolayer adsorption onto the homogenous surface [53]. The Langmuir model isotherm equation can be expressed as follows:

$$\frac{c_e}{q_e} = \frac{c_e}{Q_m} + \frac{1}{K_L Q_m} \tag{6}$$

where c_e (mg/L) is the equilibrium concentration of phenols in the liquid phase, q_e (mg/g) is the adsorption capacity of the adsorbent at equilibrium, Q_m (mg/g) is the maximum adsorption capacity corresponding to complete monolayer converge, and K_L (L/mg) is Langmuir constant related to the affinity of the binding sites. R_L, an equilibrium parameter can express the essential characteristics of the Langmuir isotherm model, which is defined by the following formula [54]:

$$R_L = \frac{1}{1 + K_L c_o} \tag{7}$$

where C_0 (mg/L) is the highest initial phenol concentration, the value of R_L indicates the adsorption nature to be either irreversible adsorption ($R_L = 0$), favorable adsorption ($0 < R_L < 1$), linear adsorption ($R_L = 1$) or unfavorable adsorption ($R_L > 1$).

The Freundlich isotherm model is suitable for multilayer adsorption and heterogeneous surfaces, which can be written as:

$$\ln q_e = \ln K_f + \frac{1}{n} \ln c_e \tag{8}$$

where K_f is the Freundlich constant related to the adsorption capacity, and n is the constant related to the adsorption intensity.

The Dubinin-Radushkevich (D-R) isotherm is applied to show the nature of sorption process, physical or chemical. The equation can be represented as follows:

$$\ln q_e = \ln q_m - \beta\varepsilon^2 \tag{9}$$

$$\varepsilon = RT \ln\left(1 + \frac{1}{c_e}\right) \tag{10}$$

$$E = \frac{1}{\sqrt{2\beta}} \tag{11}$$

where q_m (mg/g) is the maximum adsorption capacity, β (mol²/kJ²) is the activity coefficient related to mean adsorption energy, ε is the Polanyi potential, *R* (8.314 J/K/mol) is the universal gas constant, T (K) is the adsorptive Kelvin temperature and *E* (kJ/mol) is the adsorption free energy.

The Temkin isotherm model contains a factor that explicitly takes into account the adsorbent–adsorbate interactions, which provides important information for phenols adsorption onto the mesoporous carbon. The Temkin isotherm model can be defined according to the following formula:

$$q_e = B_1 \ln K_T + B_1 \ln c_e \tag{12}$$

where K_T (mg/L) is the equilibrium binding constant corresponding to the maximum binding energy, $B_1 = RT/b$ (J/mol) is the Temkin constant related to the heat of sorption, *b* (J/mol) is related to the heat of adsorption.

Fig. 10 shows the adsorption isotherm models of phenols on the mesoporous carbon. The parameters of the adsorption isotherm models are given in Table 3. It can be seen that the Langmuir isotherm model ($R^2 = 0.975$ for phenol, $R^2 = 0.996$ for p-chlorophenol) gives the best fitting among adsorption isotherm models, which indicates that the adsorption of phenols may attribute to monolayer adsorption onto the homogenous surface. The separation factor values in this study are between 0 and 1, indicating that the adsorption behavior of phenols on the mesoporous carbon is favorable. Additionally, the R_L of p-chlorophenol (0.0391) is closer to 0 than phenol' s (0.0810), which agrees well with this study results.

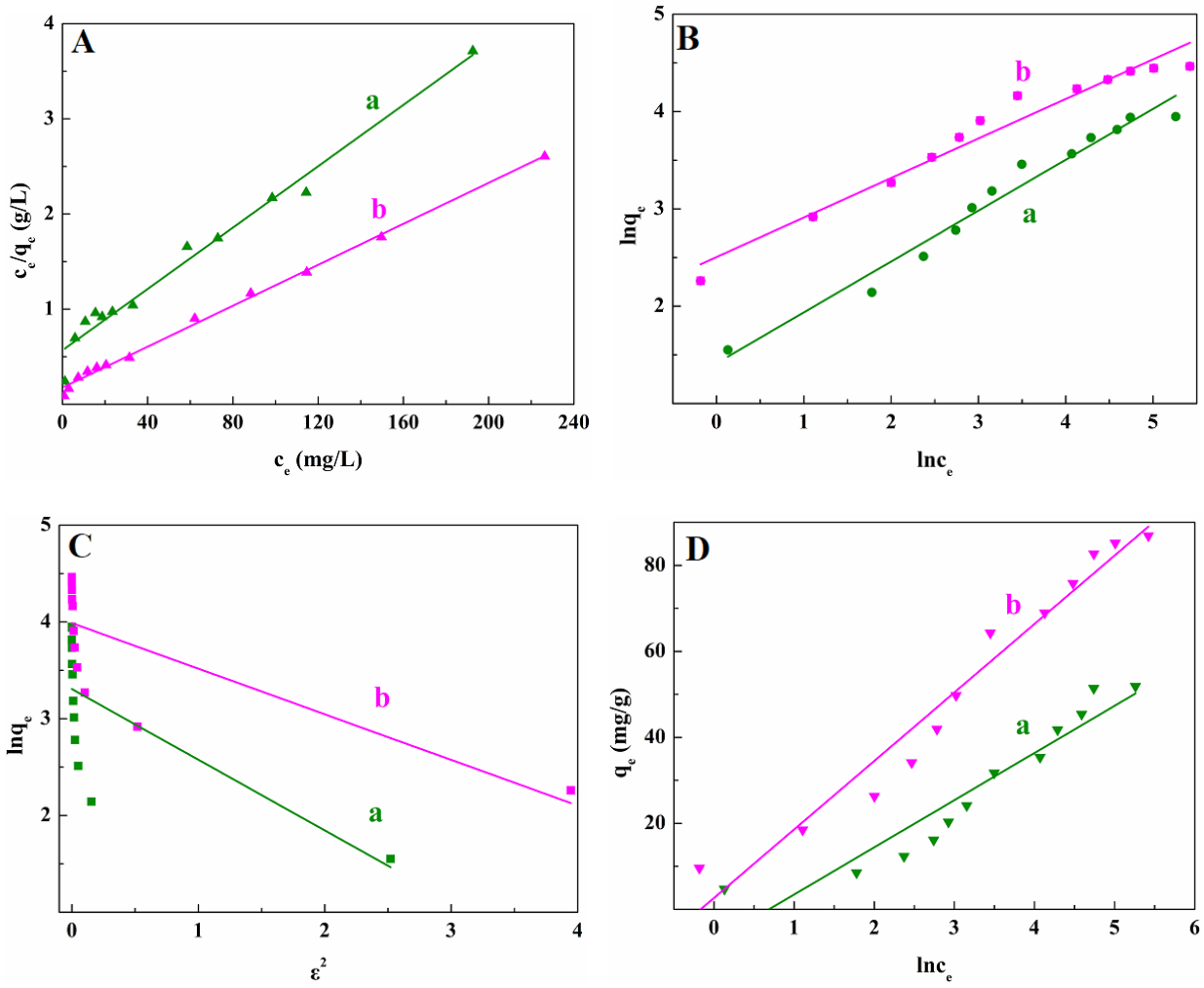

Fig. 10. The adsorption isotherms models of (a) phenol and (b) p-chlorophenol onto the TSMC A) Langmuir, B) Freundlich, C) Dubinin-Radushkevich, D) Temkin isotherms.

Table 3
Isotherm parameters for phenols adsorption onto the TSMC

Isotherm type	Isotherm parameters	Phenol	p-chlorophenol
Langmuir	Q_m (mg/g)	62.035	92.937
	K_L (L/mg)	0.0284	0.0614
	R^2	0.975	0.996
	R_L	0.0810	0.0391
Freundlich	K_f	4.110	12.237
	n	1.913	2.461
	R^2	0.968	0.957
Dubinin–Radushkevich	q_m (mg/g)	27.286	53.973
	E (kJ/mol)	0.827	1.030
	R^2	0.422	0.541
Temkin	B_1 (J/mol)	10.968	15.924
	K_T	0.504	1.181
	R^2	0.891	0.955

In this study, the Freundlich equation is not as good as the Langmuir equation to reveal the relationship between the adsorption capacity (q_e) and the equilibrium concentration (c_e), which may be derived from its assumption of heterogeneous adsorbent surface; in fact, the surface of the mesoporous carbon is relatively uniform. The values of the n (1.913 for phenol and 2.461 for p-chlorophenol, respectively) are higher than 1, which reveal the favorable adsorption.

From Table 3 it can be found that the Dubinin-Radushkevich equation gives the worst fitting in all cases, which cannot give an accurate prediction information. The R^2 values of the Temkin isotherm model are higher, thus it can also represent the experimental in a certain degree. In addition, the heat of sorption process are 10.968 J/mol for phenol and 15.924 J/mol for p-chlorophenol, respectively.

3.6. Effect of temperature and thermodynamic analyses

The temperature plays an important role in adsorption of phenols. Generally, as the temperature rises, the adsor-

bate molecule can be quickly through the adsorbate-adsorbent boundary layer and the internal of the adsorbents. Thus, the increasing temperature will improve the adsorbate molecule diffusion rate and may change the equilibrium adsorption capacity of the adsorbent [4]. In our experiment, the effect of temperature on adsorption of phenols onto the mesoporous carbon were investigated at different temperatures 20, 25, 30, 35 and 40°C. From Fig. 11, with the increase of temperature from 20 to 40°C, it can be seen that the adsorption capacity develop from 19.13 mg/g to 21.12 mg/g for phenol and 37.54 mg/g to 41.92 mg/g for p-chlorophenol, respectively, which indicate that the adsorption of phenols onto the TSMC are controlled by an endothermic reaction. However, the q_e values of p-chlorophenol show more increase than phenol's with the rise of temperature, which may be explained in terms of the hydrophobic character of phenol and p-chlorphenol (Referring to the effect of pH). As reported by other authors, the solubility of phenol and p-chlorophenol are 93 g/L and 27 g/L, respectively. The hydrophobic interaction plays an important role in the adsorption of phenols onto the TSMC, and the surface and the pore of the carbon is tendency to adsorb the molecular with higher hydrophobicity [32].

3.6.1. Adsorption thermodynamic study

The thermodynamics study can give very valuable insights into the nature of the adsorption process. These thermodynamic parameters, the Gibbs free energy change ΔG (kJ/mol), enthalpy change ΔH (kJ/mol) and entropy change ΔS (J/K/mol) can be calculated as follows [55–57]:

$$\Delta G = -RT\ln k \tag{13}$$

$$k = \frac{q_e}{c_e} \tag{14}$$

$$\Delta G = \Delta H - T\Delta S \tag{15}$$

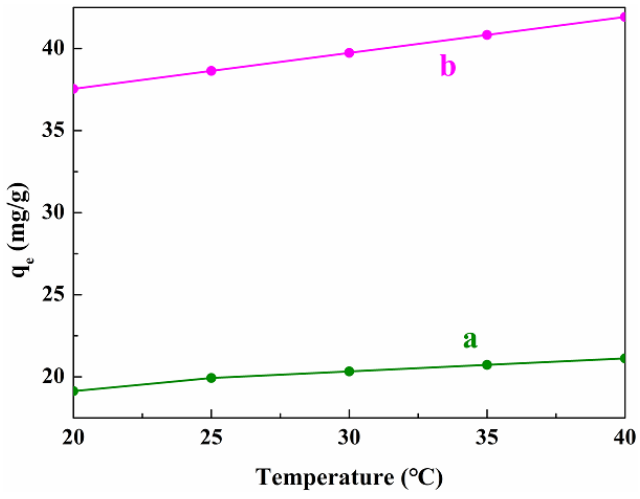

Fig. 11. Effect of the temperature on the adsorption of (a) phenol and (b) p-chlorophenol (C_o: 100 mg/L, V: 50 mL, Adsorbent dosage: 0.2 g for phenol, 0.1 g for p-chlorophenol, The initial pH 6.80 and 6.70 for phenol and p-chlorophenol, respectively).

$$\ln k = \frac{\Delta S}{R} - \frac{\Delta H}{RT} \tag{16}$$

where T (K) is the adsorptive Kelvin temperature, R (8.314 J/K/mol) is the universal gas constant, k is the adsorption equilibrium constant.

The calculated values (Fig. 12) of the Gibbs free energy change, enthalpy change and entropy change of phenols are summarized in Table 4. Generally, the values of ΔG are between –20 and 0 kJ/mol for physisorption, but chemisorption is a range of –80 to –400 kJ/mol [41]. The values of ΔG are negative for p-chlorophenol, corresponding to a spontaneous physical process. Meanwhile, the ΔG values of phenol are in the range of 0.437 to –0.826 kJ/mol, indicating that the adsorption of phenol onto the TSMC is mainly physical. The magnitude of the ΔH values lie in the range of 2.1–20.9 and 80–200 kJ/mol for physical and chemical adsorptions, respectively [58]. From Table 4, the ΔH values of phenols are positive, being due to the fact that some carbons need a bigger amount of energy to remove water molecules from their pores, which also clearly demonstrates the endothermic physical nature of the adsorption process [59]. On the other hand, the ΔH values of phenol and p-chlorophenol are 18.944 and 20.6715 kJ/mol, respectively, whose absolute values decrease with the increase of

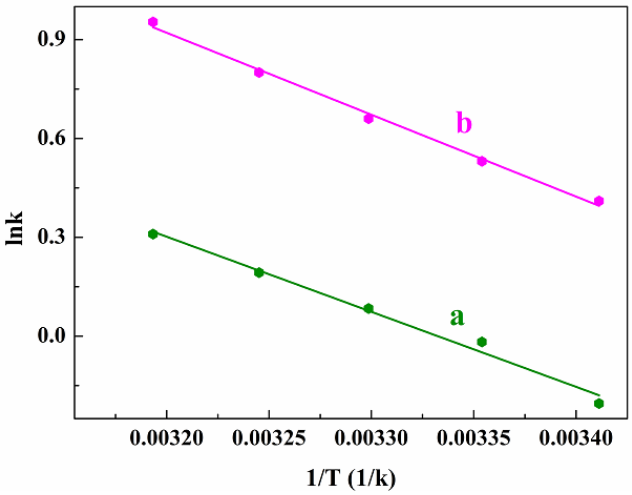

Fig. 12. The adsorption thermodynamic study of (a) phenol and (b) p-chlorophenol onto the TSMC.

Table 4
Thermodynamic parameters for phenols adsorption onto the TSMC

Parameters	Temperature	Phenol	p-chlorophenol
ΔG (kJ/mol)	293.15 (K)	0.437	–0.964
	298.15 (K)	0.121	–1.333
	303.15 (K)	–0.194	–1.702
	308.15 (K)	–0.510	–2.071
	313.15 (K)	–0.826	–2.440
ΔH (kJ/mol)		18.944	20.671
ΔS (J/mol/K)		63.132	73.804

substitution degree (Cl group for p-chlorophenol), indicating the reinforcement of physical adsorption [41]. It also can be seen that the ΔS values of phenol and p-chlorophenol are 63.132 and 73.804 J/K/mol, respectively, which show the increased randomness of the solid-liquid interface during the sorption of phenols onto the TSMC.

3.7 Adsorption mechanism

In general, several possible mechanisms including the electron donor-acceptor complex, hydrophobic interaction, electrostatic interaction and the solvent effect involve in the adsorption of phenolic compounds on the mesoporous carbon [39].

The π-π interaction may be taken into consideration in adsorption of p-chlorophenol onto the TSMC. The introduction of -Cl group would alter the π-π interaction between p-chlorophenol and the mesoporous carbon. Especially, at pH > pKa, the π-π interaction plays an important role, due to it diminishes the repulsive electrostatic interactions between the aromatic rings and the mesoporous carbon surface, which is another reason for the enhanced adsorption of the p-chlorophenol onto the TSMC. As suggested by other studies, it is possible that the adsorption of p-chlorophenol onto single-walled carbon nanotubes through π-π interaction [32]. For phenol, according to the recently report, the adsorption phenol onto the activated carbon limits any available π-π interaction [60].

The hydrophobic interaction makes contribution to the adsorption of phenols. In this study, the phenols with high hydrophobicity have stronger tendency to be adsorbed and retain on the surface or in the pores of the TSMC. Especially, the higher hydrophilicities of p-chlorophenol corresponds to a better adsorption capacity. According to previous reports, the hydrophilicities of phenols reinforced with the substitution degree increase of phenols, which resulted to the enhanced adsorption capacity of the substituted phenols onto the mesoporous carbon [41].

The molecular dimensions also have some implications on the adsorption. In the adsorption kinetics study, the phenols exhibit different initial adsorption rates due to the widest molecular dimension. Generally, the molecular size of the phenols and the average pore size of the mesoporous carbon are at the same magnitude, which could enhance the adsorption capacity of phenols. This mechanism was also reported by other authors [61].

H-bonding makes contribution to the adsorption of phenols onto the TSMC, which exists between phenols and functional groups of the TSMC. That has been discussed in the effect of adsorbent dosage part. For p-chlorophenol, the -Cl group and the -OH group could form H-bonding with C-O and -OH surface sites of the mesoporous carbon; with regard to phenol, the -OH as H-bond donor is combination with C-O or -OH as H-bond acceptors. The similar mechanism was described in Hui Yuan's study [4].

In the presence of ions, Electrostatic interaction may be the key factor during the adsorption process, which is obviously affected by the pH of solution. Phenol and p-chlorophenol are both weak acids, being dissociated at pH > pKa, which is 9.89 and 9.41 for phenol and p-chlorophenol, respectively, (the details have been discussed in the effect of pH). Therefore this kind of interaction is considered to be important in the adsorption of phenols on the mesoporous carbon. Similar mechanism was reported for phenol (2-nitrophenol) adsorption on coconut shell activated carbon (CSAC) and magnetic coconut shell activated carbon (MCSAC) [62].

Table 5
Adsorption capacity (mg/g) of regenerated TSMC to phenols for three times

Compounds	q_{e0}	q_{e1}	q_{e2}	q_{e3}
Phenol	21.13	20.99	21.15	20.89
p-chlorophenol	44.11	44.08	44.13	43.72

3.8. Regeneration of TSMC

The regeneration performance of adsorbents is essential in the development of adsorbents on an industrial scale, and an excellent desorption process should restore the adsorbents close to their initial properties, for effective reuse. The objective is realized in this study of adsorption-desorption cycles, and the remove capacity of phenols onto the TSMC at every cycle was calculated as shown in Table 5. It is clearly to observe that almost no loss of the remove capacity could be measured when up to three additional adsorption-desorption experiments were performed, indicating the TSMC has great potential for industrial applications.

4. Conclusion

In summary, the TSMC was successfully synthesized by using silica KIT-6 as the template, sucrose as the carbon precursor and subsequently carbonized at the temperature of 900°C, and the adsorption capacity of phenol and p-chlorophenol onto the TSMC were also studied. The key influence factors were investigated in detail, and the experimental results showed that the optimal conditions for the uptake of phenols onto the TSMC were as follows: the dosage of 0.2 g and 0.1 g for phenol and p-cholorophenol, the initial pH 6.80 and 6.70 for phenol and p-chlorophenol, respectively, the equilibrium time of 120 min, the solution concentration of 100 mg/L and the adsorption temperature of 30°C. The results also indicated that the adsorption process was spontaneous and endothermic. Besides, the adsorption process fitted well with the Langmuir isotherm model, and the adsorption kinetic study could be described by the pseudo-second order kinetic model. The adsorption mechanism is a complex process that includes a combination of π-π interaction, the hydrophobic interaction, the molecular dimensions, H-bonding and other interactions on the adsorption process After three repeated adsorption-desorption cycles, the TSMC retained almost the same adsorption ability, indicating excellent reusability of TSMC for phenols adsorption.

Acknowledgements

This work was supported by the National Natural Science Foundation of China (21203136), the Scientific and

Technological Innovation Programs of Higher Education Institutions in Shanxi (2015135), and the Shanxi Provincial Key Research and Development Plan (general) Social Development Project (201703D321009-5).

References

[1] A. Kuleyin, Removal of phenol and 4-chlorophenol by surfactant-modified natural zeolite, J. Hazard. Mater., 144 (2007) 307–315.

[2] X. Liu, J.H. Fan, L.M. Ma, Elimination of 4-chlorophenol in aqueous solution by the bimetallic Al-Fe/O_2 at normal temperature and pressure, Chem. Eng. J., 236 (2014) 274–284.

[3] S.H. Lin, R.S. Juang, Adsorption of phenol and its derivatives from water using synthetic resins and low-cost natural adsorbents: A review, J. Environ. Manage., 90 (2009) 1336–1349.

[4] H. Yuan, Q.L. You, L.J. Song, G.Y. Liao, H. Xia, D.S. Wang, Preparation of carbon nanotubes/porous polyimide composites for effective adsorption of 2, 4-dichlorophenol, RSC Adv., 6 (2016) 95825–95835.

[5] W.P. Cheng, W. Gao, X. Cui, J.H. Ma, R.F. Li, Phenol adsorption equilibrium and kinetics on zeolite X/activated carbon composite, J. Taiwan. Inst. Chem. Eng., 62 (2016) 192–198.

[6] C. Scully, G. Collins, V. O'Flaherty, Anaerobic biological treatment of phenol at 9.5–15 degrees C in an expanded granular sludge bed (EGSB)-based bioreactor, Water Res., 40 (2006) 3737–3744.

[7] G.B. Seetharam, B.A. Saville, Degradation of phenol using tyrosinase immobilized on siliceous supports, Water Res., 37 (2003) 436–440.

[8] K. Lin, J. Pan, Y. Chen, R. Cheng, X. Xu, Study the adsorption of phenol from aqueous solution on hydroxyapatite nanopowders, J. Hazard. Mater., 161 (2009) 231–240.

[9] Y. Park, G.A. Ayoko, E. Horváth, R. Kurdi, J. Kristof, R.L. Frosta, Structural characterisation and environmental application of organoclays for the removal of phenolic compounds, J. Colloid Interface Sci., 393 (2013) 319–334.

[10] S.K. Nadavala, K. Swayampakula, V.M. Boddu, K. Abburi, Biosorption of phenol and o-chlorophenol from aqueous solutions on to chitosan-calcium alginate blended beads, J. Hazard. Mater., 162 (2009) 482–489.

[11] N.S. Kumar, K. Min, Phenolic compounds biosorption onto Schizophyllum commune fungus: FTIR analysis, kinetics and adsorption isotherms modeling, Chem. Eng. J., 168 (2011) 562–571.

[12] P.T. Huong, B.K. Lee, J. Kim, Improved removal of 2-chlorophenol by a synthesized Cu-nano zeolite, Process Saf. Environ., 100 (2016) 272–280.

[13] T.A. Saleh, S.O. Adio, M. Asif, H. Dafalla, Statistical analysis of phenols adsorption on diethylenetriamine-modified activated carbon, J. Clean. Prod., 182 (2018) 960–968.

[14] N.S. Kumar, A.S. Reddy, V.M. Boddu, A. Krishnaiah, Development of chitosan-alginate based biosorbent for the removal of p-chlorophenol from aqueous medium, Toxicol. Environ. Chem., 91 (2009) 1035–1054.

[15] S.K. Nadavala, H.C. Man, H.S. Woo, Biosorption of phenolic compounds from aqueous solutions using Pine (Pinus densiflora Sieb) Bark Powder, BioResources, 9 (2014) 5155–5174.

[16] N.S. Kumar, K. Min, Removal of phenolic compounds from aqueous solutions by biosorption onto acacia leucocephala bark powder: equilibrium and kinetic studies, J. Chil. Chem. Soc., 56(1) (2011) 539–545.

[17] Y. Zhou, L. Tang, G. Yang, G. Zeng, Y. Deng, B. Huang, Y. Cai, J. Tang, J. Wang, Y. Wu, Phosphorus–doped ordered mesoporous carbons embedded with Pd/Fe Bimetal Nanoparticles for the dechlorination of 2, 4–dichlorophenol, Catal. Sci. Technol., 6 (2016) 1930–1939.

[18] M.Z. Momčilović, M.S. Ranđelović, A.R. Zarubica, A.E. Onjia, M. Kokunešoski, B.Z. Matović, SBA-15 templated mesoporous carbons for 2, 4-dichlorophenoxyacetic acid removal, Chem. Eng. J., 220 (2013) 276–283.

[19] W. Teng, Z. Wu, J. Fan, H. Chen, D. Feng, Y. Lv, J. Wang, A. Asiri, D. Zhao, Ordered mesoporous carbons and their corresponding column for highly efficient removal of microcystin-LR, Energ. Environ. Sci., 6 (2013) 2765–2776.

[20] A. Chen, Y. Li, Y. Yu, Y. Li, L. Zhang, H. Lv, L. Liu, Mesoporous carbonaceous materials prepared from used cigarette filters for efficient phenol adsorption and CO_2 capture, Rsc Adv., 5 (2015) 107299–107306.

[21] J. Fan, X. Ran, Y. Ren, Ordered mesoporous carbonaceous materials with tunable surface property for enrichment of hexachlorobenzene, Langmuir, 32 (2016) 9922–9929.

[22] J. Yang, Y. Jin, X. Yu, Q. Yue, High surface area ordered mesoporous carbons from waste polyester: effective adsorbent for organic pollutants from aqueous solution, J. Sol-Gel Sci. Technol., 83 (2017) 413–421.

[23] G. Yang, L. Tang, G. Zeng, Y. Cai, J. Tang, Y. Pang, Y. Zhou, Y. Liu, J. Wang, S. Zhang, W. Xiong, Simultaneous removal of lead and phenol contamination from water by nitrogen-functionalized magnetic ordered mesoporous carbon, Chem. Eng. J., 259 (2015) 854–864.

[24] A. Chen, Y. Li, Y. Yu, Y. Li, K. Xia, Y. Wang, S. Li, L. Zhang, Synthesis of hollow mesoporous carbon spheres via "dissolution capture" method for effective phenol adsorption, Carbon, 103 (2016) 157–162.

[25] L. Zuo, W. Song, T. Shi, C. Lv, J. Yao, J. Liu, Y. Weng, Adsorption of aniline on template-synthesized porous carbons, Microporous Mesoporous Mater., 200 (2014) 174–181.

[26] W. Xin, Y. Song, Mesoporous carbons: recent advances in synthesis and typical applications, J. Cheminform., 5 (2015) 83239–83285.

[27] A.B. Fuertes, G. Lota, T.A. Centeno, E. Frackowiak, Templated mesoporous carbons for supercapacitor application, Electrochim. Acta., 50 (2005) 2799–2805.

[28] K.S. Lakhi, D.H. Park, K. Al-Bahily, W. Cha, B. Viswanathan, J.H. Choy, A. Vinu, Mesoporous carbon nitrides: synthesis, functionalization, and applications, Chem. Soc. Rev., 46 (2017) 72–101.

[29] H. Cheng, H. Xue, G. Zhao, Preparation, characterization, and properties of graphene-based composite aerogels via in situ polymerization and three-dimensional self assembly from graphene oxide solution, RSC Adv., 6 (2016) 78538–78547.

[30] G. Wang, S. Chen, X. Quan, H. Yu, Y. Zhang, Enhanced activation of peroxymonosulfate by nitrogen doped porous carbon for effective removal of organic pollutants, Carbon, 115 (2017) 730–739.

[31] J. Gao, X. Wang, Q. Zhao, Y. Zhang, J. Liu, Synthesis and supercapacitive performance of three-dimensional cubic-ordered mesoporous carbons, Electrochim. Acta., 163 (2015) 223–231.

[32] H. Ding, X. Shen, C. Chen, X. Zhang, Molecular dynamics simulations of simple aromatic compounds adsorption on single-walled carbon nanotubes, RSC Adv., 6 (2016) 80972–80980.

[33] K. Babaeivelni, A.P. Khodadoust, Adsorption of fluoride onto crystalline titanium dioxide: Effect of pH, ionic strength, and co-existing ions, J. Colloid Interface Sci., 394 (2013) 419–427.

[34] J.C. Lazo-Cannata, A. Nieto-Marquez, A. Jacoby, A.L. Paredes-Doig, A. Romero, M.R. Sun-Kou, J. Valverde, Adsorption of phenol and nitrophenols by carbon nanospheres: Effect of pH and ionic strength, Sep. Purif. Technol., 80 (2011) 217–224.

[35] L. Zhu, A. Baoliang Chen, X. Shen, Sorption of phenol, P-nitrophenol, and aniline to dual-cation organobentonites from water, Environ. Sci. Technol., 34 (2000) 16–19.

[36] L.S. Guinesi, E.T. Gomes Cavalheiro, Influence of some reactional parameters on the substitution degree of biopolymeric Schiff bases prepared from chitosan and salicylaldehyde, Carbohydr. Polym., 65 (2006) 557–561.

[37] M. Kragulj, J. Trickovi, A. Kukovecz, B. Jovic, J. Molnar, S. Roncevi, Z. Konya, B. Dalmacija, Adsorption of chlorinated phenols on multiwalled carbon nanotubes, RSC Adv., 5 (2015) 24920–24929.

[38] J. Li, X. Meng, C. Hu, J. Du, Adsorption of phenol, p-chlorophenol and p-nitrophenol onto functional chitosan, Bioresour. Technol., 100 (2009) 1168–1173.

[39] C. Moreno-Castilla, Adsorption of organic molecules from aqueous solutions on carbon materials, Carbon, 42 (2004) 83–94.
[40] Q. Lu, G.A. Sorial, The effect of functional groups on oligomerization of phenolics on activated carbon, J. Hazard. Mater., 148 (2007) 436–445.
[41] Q. Liu, T. Zheng, P. Wang, J. Jiang, N. Li, Adsorption isotherm, kinetic and mechanism studies of some substituted phenols on activated carbon fibers, Chem. Eng. J., 157 (2010) 348–356.
[42] M.D. Víctor-Ortega, J.M. Ochando-Pulido, A. Martínez-Férez, Phenols removal from industrial effluents through novel polymeric resins: Kinetics and equilibrium studies, Sep. Purif. Technol., 160 (2016) 136–144.
[43] X. Yang, M. Guo, Y. Wu, Q. Wu, R. Zhang, Removal of emulsified oil from water by fruiting bodies of macro-fungus, Plos One, 9 (2014) 162–195.
[44] N. Yeddou, A. Bensmaili, Kinetic models for the sorption of dye from aqueous solution by clay-wood sawdust mixture, Desalination, 185 (2005) 499–508.
[45] W.J. Weber, J.C. Morris, Kinetics of adsorption on carbon from solution, J. Sanit. Eng. Div., 1 (1963) 1–2.
[46] S. Altenor, B. Carene, E. Emmanuel, J. Lambert, J.-J. Ehrhardt, S. Gaspard, Adsorption studies of methylene blue and phenol onto vetiver roots activated carbon prepared by chemical activation, J. Hazard. Mater., 165 (2009) 1029–1039.
[47] M. Sharma, R.K. Vyas, K. Singh, Theoretical and experimental analysis of reactive adsorption in a packed bed: parallel and branched pore-diffusion model approach, Ind. Eng. Chem. Res., 55 (2016) 5945–5954.
[48] C.T. Hsieh, H. Teng, Influence of mesopore volume and adsorbate size on adsorption capacities of activated carbons in aqueous solutions, Carbon, 38 (2000) 863–869.
[49] I. Langmuir, The adsorption of gases on plane surfaces of glass, mica and platinum, J. Chem. Phys., 40 (1918) 1362–1403.
[50] M.D. Levan, T. Vermeulen, Binary Langmuir and Freundlich isotherms for ideal adsorbed solutions, J. Phys. Chem., 85 (1981) 3247–3250.
[51] V. Gianotti, M. Benzi, G. Croce, P. Frascarolo, F. Gosetti, E. Mazzucco, M. Bottaro, M. Gennaro, The use of clays to sequestrate organic pollutants: Leaching experiments, Chemosphere, 73 (2008) 1731–1736.
[52] C. Aharoni, M. Ungarish, Kinetics of activated chemisorption. Part 2.-Theoretical models, J. Chem. Soc. Faraday Trans., 73 (1977) 456–464.
[53] Z. Noorimotlagh, R.D.C. Soltani, A.R. Khataee, S. Shahriyar, H. Nourmoradi, Adsorption of a textile dye in aqueous phase using mesoporous activated carbon prepared from Iranian milk vetch, J. Taiwan. Inst. Chem. Eng., 45 (2014) 1783–1791.
[54] Z. Luo, M. Gao, S. Yang, Q. Yang, Adsorption of phenols on reduced-charge montmorillonites modified by bispyridinium dibromides: Mechanism, kinetics and thermodynamics studies, Colloids Surf. A, 482 (2015) 222–230.
[55] P.S. Nayak, B.K, Singh, Removal of phenol from aqueous solutions by sorption on low cost clay, Desalination, 207 (2007) 71–79.
[56] A.A. Khan, R.P. Singh, Adsorption thermodynamics of carbofuran on Sn (IV) arsenosilicate in H^+, Na^+ and Ca^{2+} forms, Colloids Surf., 24 (1987) 33–42.
[57] L. Zhu, X. Ren, S. Yu, Use of cetyltrimethyl ammonium bromide-bentonite to remove organic contaminants of varying polar character from water, Environ. Sci. Technol., 32 (1998) 3374–3378.
[58] Y. Liu, Is the free energy change of adsorption correctly calculated? J. Chem. Eng. Data, 54 (2009) 1981–1985.
[59] B. Pardo, N. Ferrer, J. Sempere, R. Gonzalez-Olmos, A key parameter on the adsorption of diluted aniline solutions with activated carbons: The surface oxygen content, Chemosphere, 162 (2016) 181–188.
[60] C.Y. Yin, M.F. Ng, B.M. Goh, M. Saunders, N. Hill, Z.T. Jiang, J. Balach, M. El-Harbawi, Probing the interactions of phenol with oxygenated functional groups on curved fullerene-like sheets in activated carbon, Phys. Chem. Chem. Phys. Pccp., 18 (2016) 3700–3705.
[61] E. Lorenc-Grabowska, M.A. Diez, G. Gryglewicz, Influence of pore size distribution on the adsorption of phenol on PET-based activated carbons, J. Colloid Interface Sci., 469 (2016) 205–212.
[62] A. Sarswat, D. Mohan, Sustainable development of coconut shell activated carbon (CSAC) and magnetic coconut shell activated carbon (MCSAC) for phenol (2-nitrophenol) removal, RSC Adv., 6 (2016) 85390–85410.

Supporting Information

Table S1
The experimental data of the effect of TSMC dosage on the adsorption of phenol and p-chlorophenol

Dosage (g)	Phenol		p-chlorophenol	
	Remove (%)	q_e (mg/g)	Remove (%)	q_e (mg/g)
0.02	–	–	31.311	78.278
0.05	–	–	61.956	69.956
0.08	–	–	79.466	49.666
0.10	70.146	35.073	88.222	44.111
0.15	74.932	24.977	90.411	30.137
0.20	84.503	21.126	90.411	22.603
0.25	87.694	17.539	90.411	18.082
0.30	90.884	15.147	90.411	15.068
0.35	90.884	12.983	–	–
0.40	90.884	11.360	–	–
0.45	90.884	10.098	–	–

Table S2
The experimental data of the effect of solution pH on the adsorption of phenol and p-chlorophenol onto the TSMC

pH	phenol	p-chlorophenol
	q_e (mg/g)	q_e (mg/g)
2.0	22.721	45.205
4.0	21.923	41.922
6.0	20.727	40.828
8.0	20.727	40.827
9.0	20.727	38.639
10.0	20.727	34.261
11.0	19.132	30.978
12.0	14.346	27.694

Table S3
The experimental data of the effect of contact time on the adsorption of phenol and p-chlorophenol onto the TSMC

Time (min)	Phenol	p-chlorophenol
	q_e (mg/g)	q_e (mg/g)
5	14.346	10.184
10	17.935	21.128
15	18.733	24.411
20	19.132	26.600
30	19.531	29.883
40	20.328	34.261
60	21.126	37.544
80	21.126	39.733
100	21.525	39.733
120	21.525	40.828
150	21.923	40.828
180	21.923	40.828
240	21.923	41.922

Table S4
The experimental data of the effect of initial concentration on the adsorption of phenol and p-chlorophenol onto the TSMC

c_0 (mg/L)	Phenol	p-chlorophenol
	q_e (mg/g)	q_e (mg/g)
20	4.715	9.583
40	8.5187	18.489
60	12.322	26.300
80	16.126	34.111
100	20.328	41.922
120	24.132	49.733
160	31.739	64.261
200	35.358	68.939
240	41.768	75.806
280	45.387	82.673
320	51.399	85.162
400	51.857	86.856

Table S5
The experimental data of the effect of temperature on the adsorption of phenol and p-chlorophenol onto the TSMC

T (°C)	Phenol	p-chlorophenol
	q_e (mg/g)	q_e (mg/g)
20	19.132	37.544
25	19.929	38.639
30	20.328	39.733
35	20.727	40.828
40	21.126	41.922